

Modelling a turbidity maximum in a schematized estuary coupling TELEMAC-3D with GAIA

Sven Smolders¹; Diem Nguyen²
sven.smolders@mow.vlaanderen.be

¹ Flanders Hydraulics, dept. of Mobility and Public Works, Flemish Government, Antwerp, Belgium
² Antea Group, Roderveldlaan 1, 2600 Berchem, Belgium

Abstract – An existing cohesive sediment TELEMAC-3D model for the Scheldt estuary (i.e. SCALDIS MUD) is able to simulate an estuarine turbidity maximum (ETM). However, this ETM is not stable over time. Simulating longer time periods will result in the disappearing of the ETM. This model uses the SEDI3D sediment module (incorporated in the TELEMAC-3D module) to perform the cohesive sediment modelling. The SCALDIS model covers a large domain and its computation times are long. This makes model improvement using multiple test simulations very time consuming. In addition, in this complex model it is more difficult to understand the different processes that play a role in the functioning of a good cohesive sediment model. Therefore, in a next step to improve our understanding of the transport mechanisms of cohesive sediments a schematized estuary model is used first. The schematized estuary uses some geometry measurements from the Scheldt estuary to have some overlap, but does not claim to be a schematized Scheldt estuary. It is merely used as a test case to gain more experience in cohesive sediment modelling and to show that a stable ETM can be reached in a cohesive sediment model. This is the subject of this paper. In a future stage the lessons learnt will be applied back on a Scheldt estuary model like SCALDIS.

Keywords: schematized estuary, cohesive sediment, GAIA, TELEMAC-3D.

I. INTRODUCTION

Cohesive sediments play an important role in the Scheldt estuary. They form the majority of the suspended sediments in the Scheldt estuary and are important for the dynamics of tidal flats and marshes. With an increasing tidal amplitude and with sea level rise, abundant sediment is important for tidal flats and marshes to grow and follow the high water levels in the estuary. Cohesive sediments settle typically in locations with low flow, like sluice inlets, docks, depoldered areas or branches with no upstream discharge. For navigation purposes its important to keep the fairway open, docks and sluices accessible. Dredging is in this case inevitable. For an optimal dredging and disposal strategy a good understanding of sediment behavior in the estuary is necessary. As a last example, cohesive sediments tend to form flocks and suspended in the water column their concentration determines the light climate in the estuary. For good plant, algae and fauna growth abundant light penetration in the water column is necessary. A very turbid system is not desirable. Understanding the sediment budget of an estuary, understanding the flow from sediment input to output is of the

utmost importance for good estuarine morphological management.

A few years ago, Flanders Hydraulics invested in a new detailed 3D hydrodynamic model of the Scheldt estuary, called SCALDIS [1]. This was done within the framework of an integrated management plan for the upper Scheldt estuary. Based on the hydrodynamic model a sand transport and a separate cohesive sediment model [2] were built. The latter however struggled keeping sediment in the water column. Almost immediately an ETM appeared in the model and at the right location, but it was not stable. Very high sedimentation rates were noticed in the shallow areas. This included the tidal flats and the shallower parts of the navigation channel. It was thus not only a wetting and drying problem. The same problem occurred at the upstream discharge boundaries of the model where the sediment that entered the model domain immediately settled, not transporting new sediment downstream. Sedimentation rates were in the order of 1 m in two weeks, which is far from physically correct. The cohesive sediment modelling was done using the module SEDI3D, which was part of the TELEMAC-3D module. Trying all kinds of parameter settings did not improve the model results. Improvement at that time were made by using some hard coding tricks not based on any physical evidence at all. Examples are amongst other decreasing the settling velocity to almost zero at the upstream boundaries or using a wind induced bottom shear stress over the entire model domain (as was done by [3]). The latter solved the problem with the very high sedimentation rates, but then the sediment in the water column was flushed out of the estuary in the matter of days. So, it was clear this was not the good way to go for model improvement.

It was clear that when building a numerical model, staying close to the physical reality with as many parameters as possible will result in better model results and less unphysical problems to solve: for example, when using the bottom roughness coefficient as a calibration parameter, can result in very unphysical values in your model, which in turn can lead to lower or higher flow velocities, as demonstrated in [4]. A flow aligned mesh was used to minimize numerical diffusion and by doing this a higher value of the bottom roughness parameter could be used, one that was much closer to physical reality and not just a value to compensate for the loss of tidal energy in the model by numerical diffusion. This automatically leads to better representation of the flow velocities. A more uniform value of

the bottom roughness parameter over the entire model domain is also closer to the physical reality and will respond better when using it in a sediment transport model.

Present day a new module for sediment transport modelling was introduced in the open TELEMAC-MASCARET modelling package and its called GAIA. It was an incentive to also have a new look at cohesive sediment modelling in the Scheldt estuary. However, experiences from the previous effort showed that testing with a computation intensive and complex model domain, results often in long waiting times and difficult to interpret results. Starting with a smaller model with a more schematized model domain would decrease the complexity a little and computation effort a lot. Setting up this model, learning how to use GAIA and trying to reach a stable ETM are the goals for this paper and are a starting point for a new cohesive sediment model for the Scheldt estuary. Lessons learnt from the schematized estuary model will later be applied to a new cohesive sediment model for the Scheldt estuary.

This paper describes the setup of three schematized estuaries, closely related to the Scheldt estuary. It will give the results of the first computations with cohesive sediments in terms of ETM formation and stability.

II. SCHEMATIZED ESTUARY MODEL

Because the lessons learnt from the schematized estuary model will be applied to a Scheldt estuary model, geometric values of the Scheldt estuary were used to make the schematized estuary. The schematized estuary is 16 km wide at the mouth and only 50 m wide 160 km at the upstream boundary. It has no side branches. For the mesh, which consists of 38228 nodes and 69705 triangular elements in the 2D plane, the upstream part (km 100-160) was made using the Blue Kenue channel mesher. The downstream part was created with the regular mesh generator in Blue Kenue. The resolution ranges from 500 m on the downstream boundary to 6 m on the upstream boundary perpendicular to the flow and 25 m along the main flow line. The width B of the estuary exponentially declines from mouth to upstream according to equation (1), copied from [5].

$$B(x) = \exp\left(\frac{-0.027 \cdot 10^{-3}x + 1.9}{5.0 \cdot 10^{-11}x^2 - 9.2 \cdot 10^{-6}x + 1}\right) \quad (1)$$

For the bottom level three variants were used, resulting in three variants of the schematized estuary. First a linear declining bottom depth H , constant over the estuary width, was implemented. This linear relationship is given in equation (2):

$$H(x) = -0.000075x - 15 \quad (2)$$

The values of this linear relationship were calculated based on the average depth at the cross section at the mouth and at the upstream boundary of the estuary (based on 2013 bathymetry) This schematized variant will be referred to in this paper as the linear schematized estuary. It is shown in top view in Figure 1 and the bottom profile is shown in Figure 2.

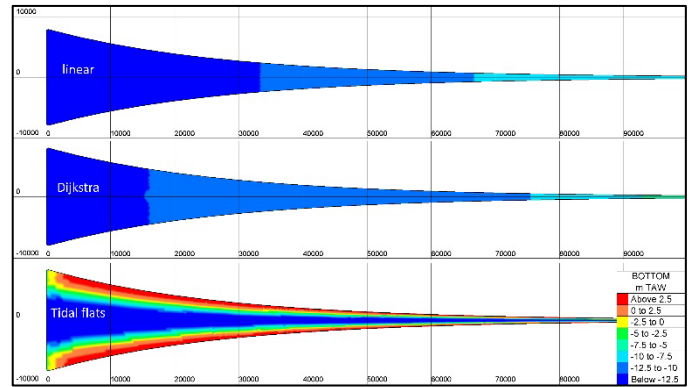


Figure 1. Shape and bottom representation of the three schematized estuaries: linear, Dijkstra and tidal flats.

For the second variant the bottom profile follows a fifth polynomial given in equation (3) and this was copied from [5]. This polynomial was fitted by [5] to Scheldt estuary data.

$$H(x) = -2.9 \cdot 10^{-24}x^5 + 1.4 \cdot 10^{-18}x^4 - 2.4 \cdot 10^{-13}x^3 + 1.7 \cdot 10^{-8}x^2 - 5.2 \cdot 10^{-4}x + 17.3 \quad (3)$$

This bottom profile is also shown in Figure 1 and Figure 2. It is referred to in this paper as the Dijkstra schematized estuary, after the name of the first author in [5]. This variant is however still very different from the version made in the iFlow model software by [5] and it is not the intention of this paper to compare both models.

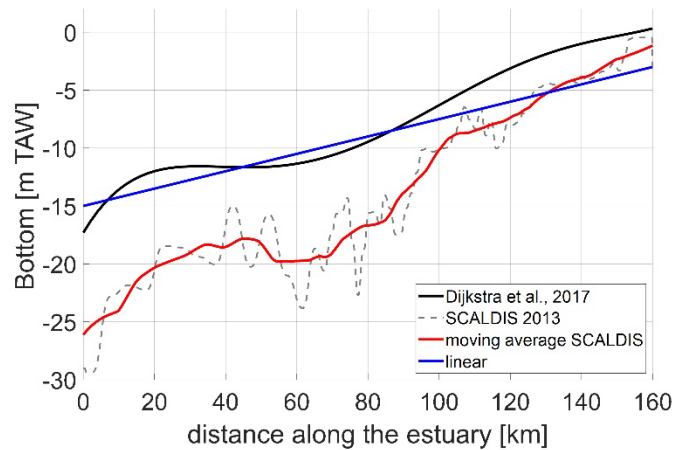


Figure 2. Bottom profiles along the estuary for the three schematized estuaries. Elevations are expressed in m TAW, where TAW is the Belgian reference level, with 0 m TAW corresponding to average low water level at sea.

For the third and last variant the bottom of the thalweg of the SCALDIS model was taken and smoothed using a moving average, clearly shown in Figure 2. However, unlike the two previous variants, this variant does not have a constant bottom over the estuary width. Tidal flats are introduced and their height varies along the length of the estuary. Intertidal measurements from the Scheldt estuary were used to determine the height of the deepest and highest point of the intertidal area in this schematized model. On average every 20 km a cross section was made with different heights, linearly interpolating in between

the cross sections. The width of the tidal flats however was always kept at 15% of the total width. Therefore, 30% of the total width of this schematized estuary is intertidal area (like some parts of the Scheldt estuary). A cross section is shown in Figure 3.

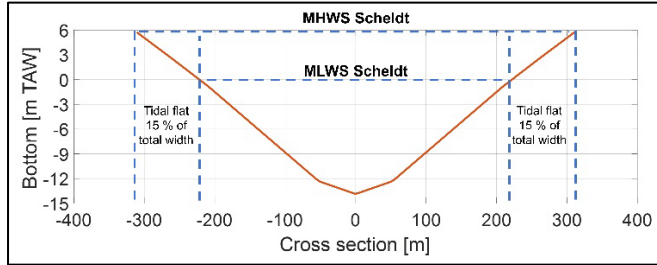


Figure 3. Schematic cross section of variant three of the schematized estuaries introducing tidal flats. Cross section at 90 km from mouth is shown with water levels of mean high water spring tide (MHWS) and mean low water spring tide (MLWS).

Although the heights vary along the estuary and coincide with the heights in the Scheldt estuary, the water level in this schematized estuary does not necessarily follow the high and low water levels of the Scheldt estuary and so the 30% intertidal area provided in the model might not be used entirely, depending on the water levels reached in the model.

Although the schematized estuaries use some or more geometric values of the Scheldt estuary, they are still very different and so it is not the intention to calibrate water levels to the water levels of the Scheldt estuary. They are considered as different estuaries with similar characteristics.

The bottom roughness is described by the Nikuradse bottom roughness value of 0,02 m for the entire model domain.

All three model variants use 15 horizontal plains evenly distributed over the depth. This brings the total node count for these models to 573420.

The downstream boundary is a water level boundary where the tides enter the model domain. Subroutine SL3 is used to describe the downstream water level at the boundary using three important tidal constituents: M2, S2 and M4 (see Table 1). Including the S2 constituent introduces the spring neap variation in the tides. Using tidal constituents to describe the boundary condition has the advantage that they can be analysed also inside the model domain and they can be changed in the future for analysing the effect of tidal asymmetry on sediment transport in the model domain. For this first exercise in this paper the boundary water level, SL3, is described by equation (4). The values for the tidal constituents are taken again from the Scheldt estuary, station Vlissingen, which lies near the mouth of the estuary. These values are kept the same for all simulations presented in this paper and values for amplitude and phase are given in Table 1.

$$SL3 = Z_0 + A_{M2} \sin(F_{M2} * t + \varphi_{M2}) + A_{M4} \sin(F_{M4} * t + \varphi_{M4}) + A_{S2} \sin(F_{S2} * t + \varphi_{S2}) \quad (4)$$

For the upstream boundary a constant discharge Q is imposed. The discharge varies between simulations from 5 m³/s to 50 m³/s and 200 m³/s. The latter two are introduced in the

model by starting with a lower value and increasing this value over the course of a few hours in the simulation for stability reasons.

Table 1. Values for de tidal forcing at the downstream boundary. Values correspond with similar values from the Scheldt estuary near Vlissingen (=mouth).

Z_0	2,31 m TAW	Reference level
A_{M2}	1,71 m	Amplitude M2
A_{M4}	0,13 m	Amplitude M4
A_{S2}	0,57 m	Amplitude S2
φ_{M2}	$66 * \pi / 180$	Phase M2
φ_{M4}	$133 * \pi / 180$	Phase M4
φ_{S2}	$114 * \pi / 180$	Phase S2
F_{M2}	$2 * \pi / (3600 * 12,42)$	Frequency M2
F_{M4}	$2 * F_{M2}$	Frequency M4
F_{S2}	$2 * \pi / (3600 * 12)$	Frequency S2

Salinity is an active tracer in the models. In the Scheldt estuary the salinity is well mixed and so for these schematized models the initial values are described by a horizontal salinity profile which ranges from salinity 30 at the mouth and decrease linearly to salinity 0 towards km 88.

The time step for the linear and Dijkstra schematized estuaries is 15 s, for the variant with tidal flats the time step is 10 s. 100 days were simulated each time and graphic output was given every 10 minutes.

For the turbulence modelling a mixing length model of Nezu and Nakagawa is used for the vertical and a constant turbulence model is used for the horizontal.

The cohesive sediment model in GAIA starts with one fraction of sediments. Initially 0,3 g/L of sediment is present in the water column. Water that enters at the downstream boundary has a sediment load of 0,02 g/L. 0,098 g/L is used for the upstream boundary. The bed is initially empty. Settling velocity is set at 0,1 mm/s. This is a good value for individual clay particles, but is an order of magnitude too low for flocks. But flocculation is not yet considered in this exercise. The critical shear stress for erosion is 0,05 N/m². The Partheniades constant or erosion constant is set at 1,5E-4. The value of the parameter for the critical shear stress for deposition is not used in these simulations, but is calculated by the code. Settling lag is turned on. The minimal value for the water depth is set to 0,1 m. These values are kept the same for all simulations shown in this paper.

In this paper only the results of five simulations are shown and discussed. All parameters are kept the same except for the upstream discharge:

- Linear schematized estuary with $Q = 50$ m³/s
- Dijkstra schematized estuary with $Q = 5, 50$ and 200 m³/s
- Tidal flats schematized estuary with $Q = 50$ m³/s

III. ETM IN THE SCHELDT ESTUARY

Four times per year a vessel sails along the Scheldt estuary following the ebb tide to measure, amongst others, the suspended sediment concentration (SSC) near the bottom and near the surface. Figure 4 shows the measurements from 2021. An ETM shows around km 110-120. With high freshwater discharges this ETM migrates downstream or is sometimes flushed entirely. In very dry conditions with very low freshwater discharge (yellow line, September 2021 in Figure 4) an additional ETM shows upstream around km 140-150. Further an ETM is seen around km 60-70. This is just downstream of Antwerp. A lot of dredging and disposal activities are carried out in this region and this ETM might be fed by the disposed dredged material. With higher winter discharges this is the first ETM to be flushed out of the estuary.

These measurements give a view on the SSC along the Scheldt estuary on four single time steps. Further 6 permanent measuring stations monitor the SSC in the estuary at fixed locations. These measurements give an idea of the fluctuation over longer periods of time and sometimes the migration of an ETM can be noticed in one of these stations.

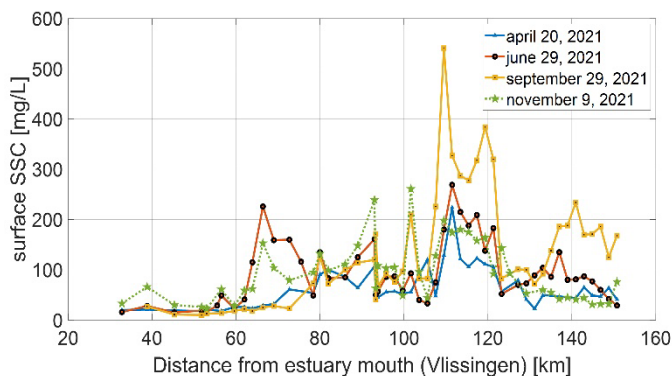


Figure 4. Measured surface suspended sediment concentrations along the Scheldt estuary for the four seasons in 2021.

From previous modelling experience the ETM furthest downstream occurs easily when dredging and disposal activities are incorporated into the model. The ETM around km 110-120 showed in the old cohesive sediment model when sufficient sediment was present. Due to high sedimentation rates upstream and the unphysical measures taken in the old model to prevent this, the most upstream ETM during low discharge periods was not yet found in the model. The exercise in this paper is however to show a stable ETM can be formed in an estuary model in TELEMAC-3D coupled with GAIA.

The different physical processes that form a turbidity maximum in estuaries, like gravitational circulation, tidal pumping, Stokes drift, scour lag and spatial settling lag are not discussed here and will not be discussed in the model results sections as this paper shows only preliminary results. Further research will need to follow.

IV. MODEL RESULTS

A. Tidal constituents

The tidal constituents imposed on the downstream boundary are known. How they evolve traveling along the estuary can be

deducted from water level time series extracting the constituents using t_{tide} from [6]. Figure 5 shows the M2, S2 and M4 amplitudes of the three schematized estuary variants for a simulation with constant upstream discharge equal to $50 \text{ m}^3/\text{s}$. For comparison the values for the Scheldt estuary are added to the figure. For all estuaries the values diverge the more upstream the location. The Dijkstra and tidal flats variant show an increase in M2 amplitude followed by a decrease near the upstream end, like in the Scheldt estuary. For all three constituents it is clear that the Dijkstra and tidal flats variant follow the trend of the Scheldt estuary the best. The difference upstream are quite large, and this is seen in the low water level behaviour much more than in the high water levels as will be shown in the next section.

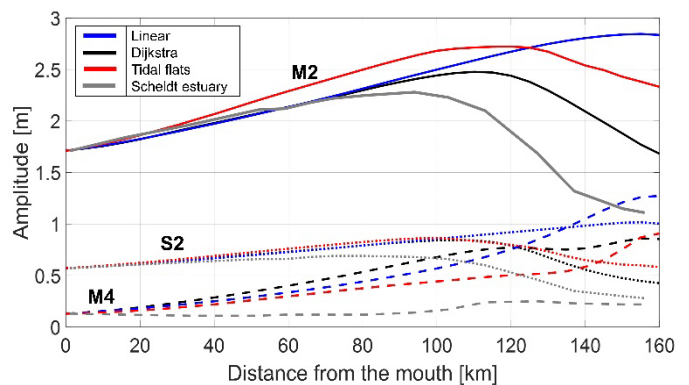


Figure 5. Comparison of the M2, S2 and M4 amplitudes of the three different modelled schematized estuaries and measured values from the Scheldt estuary. The modelled results are taken from simulations with upstream discharge $Q = 50 \text{ m}^3/\text{s}$.

B. Water levels

The maximum high water level and the minimum low water level during spring tide for the three schematized estuary variants is given in Figure 6. For the Dijkstra variant three different water levels are given for three different upstream discharges, i.e. for 5, 50 and $200 \text{ m}^3/\text{s}$. The higher the discharge the higher the water level (low and high) upstream. The influence of the discharge on the water levels reaches approximately 45 km downstream. The linear variant has the highest tidal range upstream the estuary, followed by the tidal flats variant.

Despite the differences in bottom level being quite high between the schematized estuary variants, the high and low water levels remain close to each other in the downstream part of the estuaries. At least it seems that way in Figure 6 because of the large scale on the y-axis. The differences reach up to 20 cm with the tidal flats variant having the highest high water levels downstream and the linear variant the lowest high water levels. For the low water levels the tidal flats variant has the lowest water levels and the linear variant the highest, giving the tidal flats variant the highest tidal range in the downstream part of the estuary.

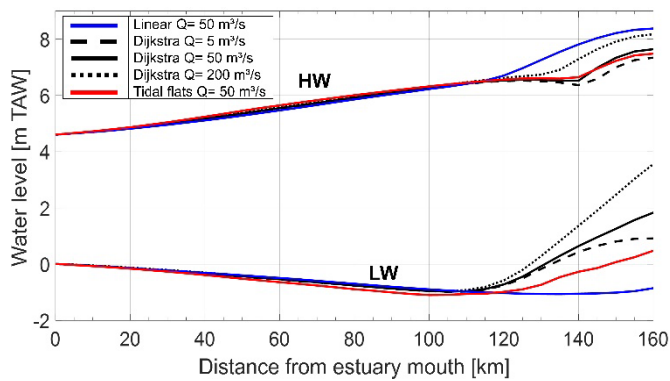


Figure 6. High (HW) and Low (LW) water levels during spring tide in the different schematized estuaries for different upstream discharges Q.

C. Cohesive sediment

After 100 simulated days the suspended sediment concentration in the water column along the central axis x of the estuary is plotted to see if an ETM occurs and to see the differences between the variants and the difference within one variant with different upstream discharges. The results are plotted in Figure 7. Compared to the linear and Dijkstra variant the tidal flats variant shows still a distinct area with increased suspended sediment concentration, but the values are much lower. All found ETM's are found relatively stable as they did not change much in the last 20 days of the simulation. For the Dijkstra variant the differences in upstream discharge show that with higher discharges the ETM is narrower and situated more downstream.

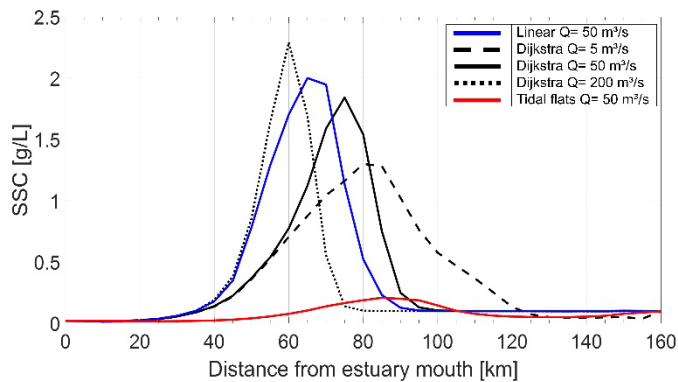


Figure 7. SSC values [g/L] for the three schematized estuaries after 100 simulated days. The results show maximum SSC values during spring tide, during flood.

The SSC values for the linear and Dijkstra variant are however far above the measured values of ETM of just SSC values in the Scheldt estuary (see Figure 4). Looking in detail to only the results of the tidal flats variant in Figure 8 it shows that SSC values are in the same order of magnitude as the measured values in the Scheldt estuary. With the y-axis scale in Figure 8 a clear ETM is visible around km 60-110. The range of this ETM along the central estuary axis is quite large. The sediment transport over several transects (0, 20, 40, 60, 80, 100, 120, 140 km) was calculated for each time step of the last full spring neap tidal cycle and averaged. This is called the averaged sediment flux and is expressed in kg/s. negative values indicate a net

downstream transport and positive values a net upstream transport. They are represented by red and green arrows respectively in Figure 8. This shows that there is a large input on the downstream boundary. The sediment load in the water column there is small but the volume of water is large, resulting in a large sediment input. In the region of the ETM there is a net upstream transport of sediment. Further downstream and upstream there is a net downstream transport. The flux of sediment entering the estuary upstream is 5 kg/s. However, in the first cross section downstream this value drops significantly, showing that most of the sediment entering the estuary upstream remains in the upstream section. This is a point of attention for further improvement as this is caused by the boundary itself (low flow velocities entering the estuary).

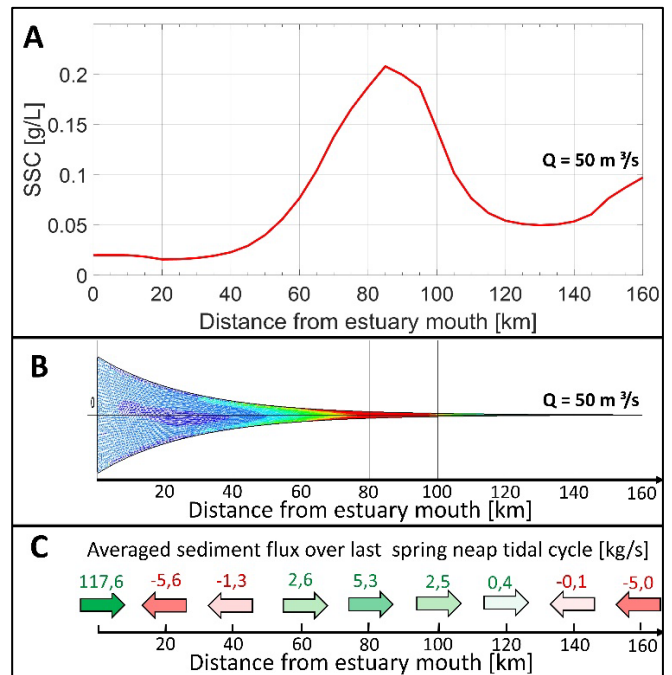


Figure 8. A. SSC values along the tidal flats schematized estuary variant after 100 simulated days; B. SSC values shown in top view of the model; C. the sediment fluxes averaged over the last spring neap tidal cycle are given in green (upstream transport) and red (downstream transport) arrows for transects every 20 km.

The same evaluations are made for the different discharges of the Dijkstra variant. The averaged fluxes and representing arrows are shown in Figure 9. For the $Q = 50 \text{ m}^3/\text{s}$ scenario only one section in the middle of the estuary is showing an upstream sediment transport flux (compared to four sections in the tidal flats variant above). When the upstream discharge is very low, from km 80 and upstream the sediment transport is directed in the upstream direction. The higher values of fluxes entering at the downstream boundary, compared to the tidal flats variant are due to the fact that the model water volume of the Dijkstra variant is almost double of that from the tidal flats variant and this causes the entrance of a much larger sediment volume at the downstream entrance for the Dijkstra variant. Increasing the upstream discharge to $200 \text{ m}^3/\text{s}$ will point all fluxes at all transects in the downstream direction. This means that eventually the ETM will disappear and the sediment will settle in the mouth region. The upstream discharge did not affect

the flux direction in the downstream part (under 60 km) of the estuary. There the arrows remained pointed in the downstream direction. The tidal volume in this variant is much higher than that of the tidal flats variant or the Scheldt estuary, which makes that higher discharge values are needed to influence it. However, usually a higher discharge points the net sediment transport in downstream direction and in the Dijkstra variant it already pointed in the downstream direction. It is worth investigating how different discharge values influence the sediment transport direction in the tidal flats variant.

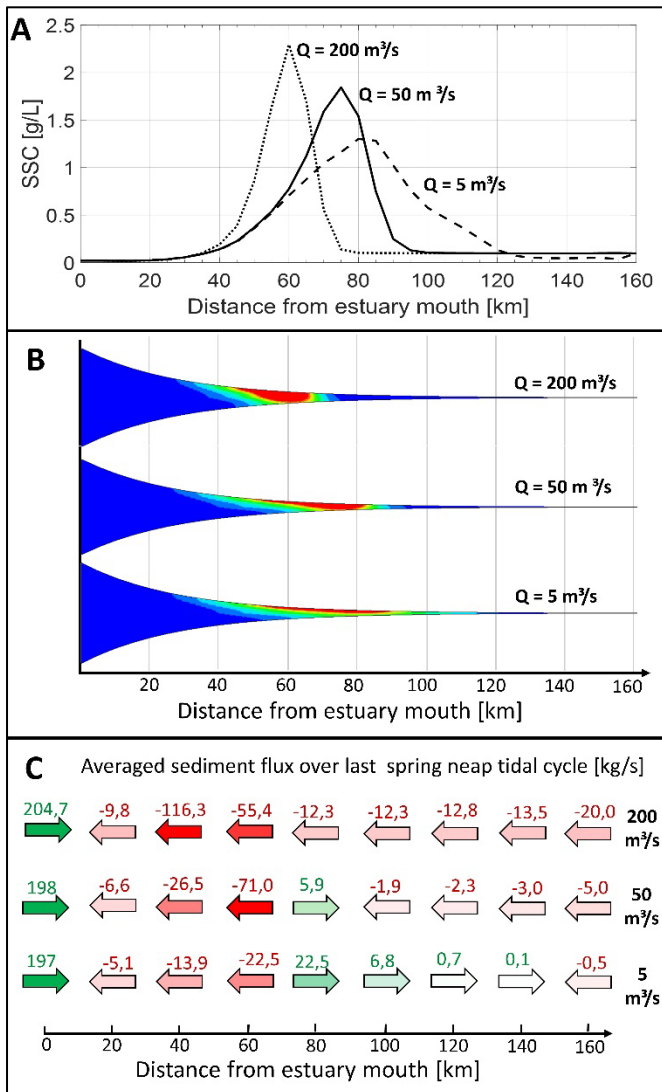


Figure 9. A. SSC values along the Dijkstra schematized estuary variant after 100 simulated days for three different upstream discharges: 200, 50 and 5 m^3/s .; B. SSC values shown in top view of the model for the different upstream discharges; C. the sediment fluxes averaged over the last spring neap tidal cycle are given in green (upstream transport) and red (downstream transport) arrows for transects every 20 km for three different upstream discharges.

With the given fluxes some parts of the models, where more sediment is flushed downstream compared to the amount of sediment that enters from upstream, or part where there is a downstream flux on the downstream side and an upstream flux on the upstream side, will run out of sediment. In these

simulations this process appears to evolve slowly, making the formed ETM's seem stable over a shorter period of time. This might be due to the constant parameter values and the low settling velocity. A higher settling velocity will have a larger effect on some of the ETM forming processes and dynamics. Despite this, ETM showing quite stable values after 100 simulated days is already a good step forward compared to the old SCALDIS mud model, where sediment settled or was flushed in a 30 day period.

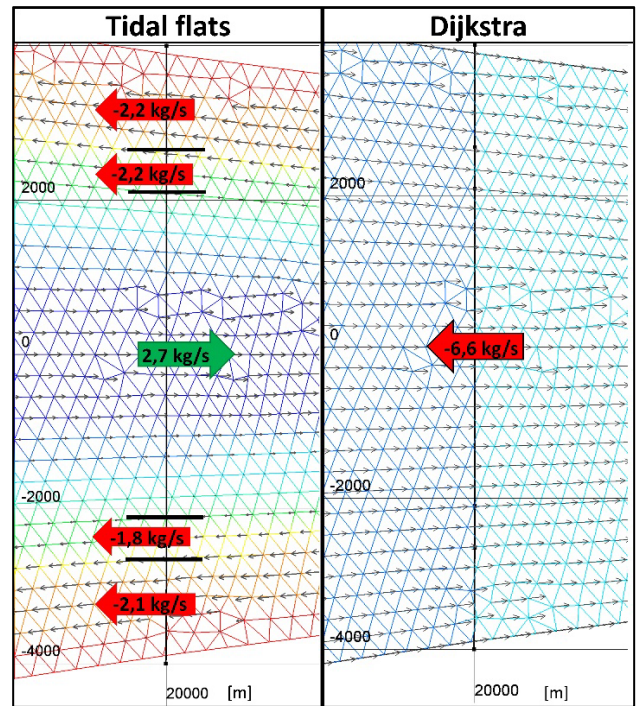


Figure 10. Comparing flow velocity direction at the end of flood for the tidal flats and Dijkstra schematized estuary variants. For the tidal flats variant the averaged fluxes over the last spring neap tidal cycle are given for parts of the 20 km transect.

The three variants of the schematized estuary model are quite different. Sometimes they give a comparable result, suggesting they act similar, but further analysis reveals big differences in processes. One example is the downstream sediment flux at the transect of km 20. The Dijkstra and tidal flats variant both give a negative flux of around 5 to 6 kg/s . Figure 10 shows the flow velocity direction at the end of flood tide. In the tidal flats variant a strong current starts to form on the tidal flats and shallower areas in the downstream direction, while the flow velocity in the deep main channel still points towards upstream. Analysing averaged sediment fluxes over parts of the transect reveals that in the deep main channel the net sediment transport is pointed upstream and the parts above -5 m TAW have a net sediment transport pointed downstream. The downstream transport over the shallow areas is bigger than the upstream transport in the main channel, resulting in a net downstream sediment transport over the entire transect. As the bottom depth is equal over the entire width in the Dijkstra variant, this phenomenon does not occur. Flow velocities are divided differently over ebb and flood resulting in a net downstream transport over all parts of the transect.

V. CONCLUSION

The first results of modelling cohesive sediments in schematized estuaries shows promising results in ETM formation. All modelled schematized estuary variants, linear, Dijkstra and tidal flats, show the formation of an ETM that is stable over time. This was the goal of this first exercise.

More analysis and longer simulation periods will be needed to see how the ETM behaves in different situations, like sediment starvation or particles with different parameter setting (especially settling velocity). The schematized estuaries forced by tidal constituent offer the possibility to also investigate how different settings for these constituents affect sediment behaviour (through tidal asymmetry).

When the different parameter settings and their impact on the global modelling result are better understood in the schematized estuary, in a next step the lessons learnt can be translated back to a full scale Scheldt estuary model, which is the final goal of this exercise.

Finally this exercise shows that TELEMAC-3D coupled with GAIA offers possibilities to model cohesive sediments and ETM formation in estuaries.

REFERENCES

- [1] Smolders, S.; Maximova, T.; Vanlede, J.; Plancke, Y.; Verwaest, T.; Mostaert, F. (2016). Integraal plan Bovenzeeschedde: Subreport 1. SCALDIS: a 3D Hydrodynamic model for the Scheldt Estuary. WL Rapporten, 13_131. Flanders Hydraulics Research: Antwerp
- [2] Smolders, S.; Bi, Q.; Vanlede, J.; De Maerschalck, B.; Plancke, Y.; Mostaert, F. (2020). Integraal plan Boven-Zeeschedde: Sub report 6 – Scaldis Mud: a Mud Transport model for the Scheldt Estuary. Version 4.0. FHR Reports, 13_131_6. Flanders Hydraulics Research: Antwerp.
- [3] van Kessel, T.; Vanlede, J.; Bruens, A. (2006). Development of a mud transport model for the Scheldt estuary in the framework of LTV: phases 1 and 2. Versie 1.0. Delft Hydraulics/Flanders Hydraulics Research: Delft. 79 + appendices pp.
- [4] Smolders, Sven (2022): How a Flow Aligned Mesh Improves TELEMAC Model Results. In: Bourban, Sébastien E.; Pham, Chi Tuân; Tassi, Pablo; Argaud, Jean-Philippe; Fouquet, Thierry; El Kadi Abderrezak, Kamal; Gonzales de Linares, Matthieu; Kopmann, Rebekka; Vidal Hurtado, Javier (Hg.): Proceedings of the XXVIIIth TELEMAC User Conference 18-19 October 2022. Paris-Saclay: EDF Direction Recherche et Développement. S. 45-49.
- [5] Dijkstra, Y. M., Brouwer, R. L., Schuttelaars, H. M., & Schramkowski, G. P. (2017). The iFlow modelling framework v2.4: A modular idealized process-based model for flow and transport in estuaries. *Geoscientific Model Development*, 10(7), 2691-2713.
- [6] Pawlowicz, R., B. Beardsley, and S. Lentz, (2002). "Classical Tidal Harmonic Analysis Including Error Estimates in MATLAB using T_TIDE", *Computers and Geosciences*, 2002.